 doi:10.20944/preprints202203.0307.v1

Article

Response Surface Optimisation of Polydimethylsiloxane (PDMS) on Borosilicate Glass and Stainless-Steel (SS316) to Increase Hydrophobicity

Nadiah Ramlan[2], Saiful Irwan Zubairi[1] and [3]* & Mohamad Yusof Maskat[1]

[1] Department of Food Sciences, Faculty of Science & Technology, Universiti Kebangsaan Malaysia, 43600 UKM Bangi, Selangor, Malaysia
[2] Academy of Contemporary Islamic Studies, Universiti Teknologi Mara (UiTM) 40450 Shah Alam, Selangor, Malaysia
[3] Tasik Chini Research Centre (PPTC), Faculty of Science & Technology, Universiti Kebangsaan Malaysia, 43600 UKM Bangi, Selangor, Malaysia
* Correspondence: author: saiful-z@ukm.edu.my (Tel. no.: +6011-23526007)

Abstract: Particle deposition on the surface of the drying chamber poses the main drawback in the spray drying process, which reduces the product recovery and affects the quality of the product. In view of this, the potential application of chemical surface modification to produce a hydrophobic surface that reduces the powder adhesion (biofouling) on the wall of the drying chamber was investigated in this study. The hydrophobic Polydimethylsiloxane (PDMS) solution was used in the vertical dipping method at room temperature to determine the optimum coating parameters on borosilicate glass and stainless-steel substrates, which were used to mimick the wall surface of the drying chamber, to achieve highly hydrophobic surfaces. A single-factor experiment was used to define the range of the PDMS concentration and treatment duration using the Response Surface Methodology (RSM). The Central Composite Rotatable Design (CCRD) was used to study the effects of the concentration of the PDMS solution (X_1, %) and the treatment duration (X_2, hr) on the contact angle of the substrate (°), which reflected the hydrophobicity of the surface. A three-dimensional (3D) response surface was constructed to examine the influence of the PDMS concentration and treatment duration on the contact angle readings, which serve as an indicator of the surface's hydrophobic characteristic. Based on the optimisation study, the PDMS coating for the borosilicate glass achieved an optimum contact angle of 99.33° through the combination PDMS concentration: X_1 = 1% (w/v) and treatment time X_2 = 4.94 hr, while the PDMS coating for the stainless-steel substrate achieved an optimum contact angle of 98.31° with PDMS concentration: X_1 = 1% (w/v) and treatment time X_2 = 1 hr. Additionally, the infrared spectra identified several new peaks that appeared on the PDMS-treated surfaces, which represented the presence of Si-O-Si, Si-CH_3, CH_2, and CH_3 functional groups for the substrates coated with PDMS. Furthermore, the surface morphology analysis using the Field Emission Scanning Electron Microscopy (FESEM) showed the presence of significant roughness and uniform nanostructure on the surface of PDMS-treated substrates, which indicated the reduction of wettability and the potential effect on unwanted biofouling on the spray drying chamber.

Keywords: Optimisation; Surface Modification; Contact Angle; PDMS; Stainless-Steel; Borosilicate Glass

1. Introduction

The spray dryer is one of the frequently used equipment in the food industry to convert liquid sample into powder form. Given its significant importance, the reduced operating efficiency and changes in the product yield and quality due to powder deposition on the spray dryer is a major concern that needs to be addressed. The high temperature during the spray drying process also increases the tendency of the naturally amorphous

 doi:10.20944/preprints202203.0307.v1

state of the food to become sticky, which is described as the glass transition phenomenon. Thus, deposit removal is considered a significant economic and environmental burden to the industry (Huang & Goddard, 2015). Although several studies have been conducted to address this issue, including the use of carrier agents and controlling the processing parameters (Fang & Bhandari, 2012; Schuck *et al*., 2005), these methods lead to new problems that alter the quality and characteristics of the dried product.

Furthermore, the wall properties of the spray dryer at which the powder adhesion takes place play a crucial role in the product deposition mechanism. Generally, fluid adhesion on the wall of the dryer depends on the surface properties of the wall (Bhandari & Howes, 2005). A previous study by Woo *et al*. (2009) reported that the wall material significantly affects the rate of particle deposition. Moreover, the wettability properties, which demonstrate the type of interaction between the solid surface and different types of liquids, have been investigated to produce anti-stick surfaces that facilitate the cleaning surface, thus, lowering the cost of cleaning tools and the price of the product adhesion. The nature of the wettability is expressed directly through the liquid contact angle readings on the surface of the material (Wang *et al*., 2011). A contact angle above 90^{o} indicates that the surface material is hydrophobic with low wettability properties. Theoretically, the contact angle for a hydrophobic surface should not be more than 120^{o} (Arkles, 2015).

Meanwhile, silicon is a polymer that contains a siloxane bond (Si-O-Si). The terms silicon and siloxane are often interchangeable to represent the same material. While the number of siloxane bonds could vary depending on the number of organic groups and the number of oxygen atoms, siloxane can have an empirical formula ranging from $(R_3Si)_2O$ to $(RSiO_{1.5})_x$ (Katsoulis *et al*., 2017) with silicon polymers having the general formula of $(RR'SiO)_x$. When the R and R' are from the methyl group, the silicon is specifically referred to as polydimethylsiloxane (PDMS). Recently, siloxane which is the functional group of silicon has been identified as one of the promising materials that provide great hydrophobic coating due to the presence of the siloxane spinal network (Yu *et al*., 2016).

In this research, a simple surface modification treatment method was proposed to form hydrophobic surfaces through the use of the hydrophobic organic PDMS solution without any additional material at room temperature. The present study aimed to elucidate the optimum conditions for the hydrophobic surface coating process using PDMS on borosilicate glass and stainless-steel substrates. This simple surface modification by using vertical dipping method was carried out to maximise the PDMS features and decrease the powder adhesion on the spray dryer wall without the use of fluorine materials and intense drying temperatures typically used to provide hydrophobic surfaces (Wang *et al*., 2012). The optimised parameters (duration of the coating process and the concentration of the PDMS solution) for the substrate surface coating process were determined using the Response Surface Methodology (RSM) method based on the resulted contact angle values. Subsequently, the surface morphology of the optimally PDMS-treated substrates was analysed using the Field Emission Scanning Electron Microscope (FESEM), while the presence of functional groups was determined using the Fourier Transform Infrared-Attenuated Total Reflectance (FTIR-ATR).

2. Materials and Methods

2.1. Chemicals and Materials

The chemicals used in this study include Dow Corning MDX4-4159 50% Medical Grade Dispersion containing 50% active silicon dimethylsiloxane copolymer with functional amino acids in a mixture of aliphatic and isopropanol solvent (Dow Corning, US) and hexane 95% (v/v) (Merck, Germany). Meanwhile, borosilicate glass microscope slides (dimension: 25 mm (h) x 25 mm (w) x 1 mm (t)) (Quasi-S Technology Sdn. Bhd., Malaysia) and stainless-steel slides (SS316) (dimension: 25 mm (h) x 25 mm (w) x 1.2 mm (t)) (Ikhlas Resmi (M) Sdn. Bhd., Malaysia) were used as the substrates to mimic the pilot- (Buchi Mini Spray Dryer B-290) and industrial-scale spray drying chamber wall. The two

Preprints (www.preprints.org) | NOT PEER-REVIEWED | Posted: 23 March 2022 doi:10.20944/preprints202203.0307.v1

substrates were chosen as they were frequently used either at the laboratory or industrial grade to study the powder deposition on both types of material (Woo *et al*., 2009).

2.2. Experimental Design of Surface Coating via the Central Composite Rotatable Design (CCRD)

The Dow Corning MDX4-4159 50% Medical Grade Dispersion containing 50% active silicon dimethylsiloxane with functional amino acids was diluted to an appropriate working concentration of 10% (v/v) using hexane solution. The optimisation of the surface coating conditions was carried out by employing the Response Surface Methodology (RSM) using the Central Composite Rotatable Design (CCRD) with two main independent variables (X_1: PDMS concentration (%, w/v) and X_2: treatment time (hr)), which was generated autonomously using a Design-Expert software version 6.0 (**Table 1**). As presented in **Figure 1**, the vertical dipping method at room temperature was employed based on the method by Wang *et al*. (2012) with slight modifications. Following the surface modification treatment, the substrate was transferred into an oven dryer at 180 °C to evaporate the carrier solution and cure the coating materials on the substrate surface prior to the contact angle analysis. The experimental data were fitted with statistical models to produce the response surface. The models were deemed suitable when the one-way Analysis of Variance (ANOVA) is significant, the lack-of-fit test is insignificant, and the coefficient determination (R^2) is more than 0.75. The chosen models were subsequently optimised based on the optimisation criteria of the minimum PDMS concentration and treatment time, while the contact angle was set to a maximum value to achieve a superhydrophobic effect.

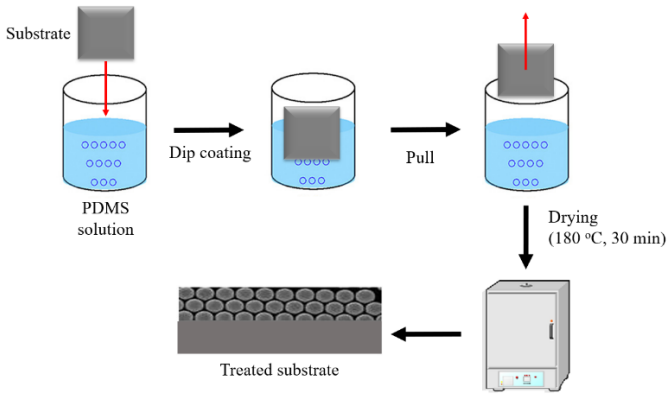

Figure 1. Procedure of the chemical treatment of the substrate surface (borosilicate glass and stainless-steel) using the PDMS solution (%, w/v) via the complete dipping method.

Table 1. Actual and coded (in parentheses) levels of PDMS concentration (X_1/x_1) and treatment time (X_2/x_2) used for optimisation of hydrophobic surface coating process on borosilicate glass and stainless-steel substrate.

Run#	X_1 (x_1) (%, w/v)	X_2 (x_2) (hr)
1	5.00 (1.000)	24.00 (1.000)
2	1.00 (-1.000)	1.00 (-1.000)
3*	3.00 (0.000)	12.50 (0.000)
4*	3.00 (0.000)	12.50 (0.000)
5*	3.00 (0.000)	12.50 (0.000)
6	3.00 (0.000)	-3.76 (-1.414)
7	3.00 (0.000)	28.76 (1.414)
8	0.17 (-1.414)	12.50 (0.000)
9	1.00 (-1.000)	24.00 (1.000)
10	5.00 (1.000)	1.00 (-1.000)
11*	3.00 (0.000)	12.50 (0.000)
12*	3.00 (0.000)	12.50 (0.000)
13	5.83 (1.414)	12.50 (0.000)

*Replication of centre point

Preprints (www.preprints.org) | NOT PEER-REVIEWED | Posted: 23 March 2022 doi:10.20944/preprints202203.0307.v1

2.3. Water Contact Angle Measurement

The water contact angle measurement was performed on the surface of the borosilicate glass and stainless-steel substrate using a Drop Shape Analyser DSA25E (Krüss, Germany) based on Sari (2006) with slight modifications, as shown in **Figure 2**. The average contact angle values were determined at five different points on the surface of the substrate (n = 5) (El Dessouky *et al*., 2017). All measurements were carried out at room temperature (28 ± 2 ˚C).

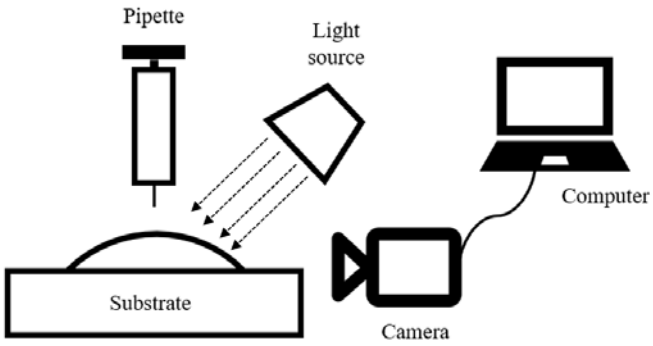

Figure 2. Experimental setup for the static contact angle measurement using the Drop Shape Analyser.

2.4. Morphological Surface Analysis: Field Emission Scanning Electron Microscopy (FESEM)

The Field Emission Scanning Electron Microscope (FESEM) (Zeiss Merlin-Compact, Germany) was used to observe the surface morphology of the coated films. Prior to the imaging at 3 kV, the samples were mounted with a double-sided adhesive carbon tape on an aluminium stub and vacuum-coated with a thin film of iridium (approximately 5.0 nm) to ensure that the samples were electrically conductive.

2.5. Functional Groups Profiling: Fourier Transform Infrared-Attenuated Total Reflectance (FTIR-ATR)

The Fourier Transform Infrared-Attenuated Total Reflectance (FTIR-ATR) spectroscopy technique was performed to identify the presence of functional groups in the borosilicate glass and stainless-steel substrates before and after the PDMS solution treatment. The FTIR analysis was performed using the FTIR/Fourier Transform Near-Infrared Spectroscopy (FT-NIR) (Perkin Elmer, United Kingdom) with a wave-number range of 4000–650 cm^{-1}.

2.6. Statistical Analysis

The Design-Expert software version 6.0.10 (Stat Ease, USA) was employed to perform the experimental design and statistical analysis. The collected data was also analysed via the ANOVA and Duncan tests using the Statistical Analytical System (SAS) version 6.12 (USA). All experiments were performed in triplicates. The optimum point was validated using the Root Mean Squared Deviation (RMSD), as shown in Equation 1 (Piñeiro *et al*., 2008):

$$RMSD = \sqrt{\frac{1}{n-1}\sum_{i=1}(\hat{y}_i - y_i)^2} \quad (1)$$

$\hat{y}_i$ = experimental value
y_i = expected value
n = number of sample

Preprints (www.preprints.org) | NOT PEER-REVIEWED | Posted: 23 March 2022 doi:10.20944/preprints202203.0307.v1

3. Results and Discussion

3.1. Optimisation of PDMS Treatment on the Stainless-steel and Borosilicate Glass

The observed response variable for the contact angle profiles of the borosilicate glass and stainless-steel surface coating treated with PDMS are shown in **Table 2**. The contact angle data were fitted using the linear, quadratic, and cubic models. Based on the statistical results, it was suggested that the modified cubic model with an inverse transformation was the most suitable model for borosilicate glass, while the modified cubic model was the most appropriate for stainless-steel substrates. The response surface equation for the contact angle data fitting based on the models are shown in **Table 3**. According to the variance analysis, both models were significant, where the R^2 value for both models was higher than 0.75, indicating a good fit. In addition, the lack-of-fit test for both substrates was insignificant, which also demonstrated a good fit between the experimental data and the model.

Table 2. Actual levels of independent variables along with the observed values for the response variables, contact angle of borosilicate glass and stainless-steel treated with PDMS.

Run#	X_1	X_2	Contact angle (°) (Y)	
			Borosilicate glass	Stainless-steel
1	**5.00**	24.00	78.48	76.72
2	1.00	1.00	90.75	97.82
3*	3.00	12.50	78.47	77.51
4*	3.00	12.50	76.74	80.53
5*	3.00	12.50	80.37	81.23
6	3.00	-3.76	82.5	83.54
7	3.00	28.76	77.02	78.16
8	0.17	12.50	87.27	90.93
9	1.00	24.00	96.69	99.93
10	5.00	1.00	81.14	76.13
11*	3.00	12.50	77.56	80.93
12*	3.00	12.50	77.23	78.92
13	5.83	12.50	88.83	91.55

Table 3. Model equations fitted for contact angle experimental data for PDMS surface coating on borosilicate glass and stainless-steel substrates.

Substrate	Response	Model equation	Model significance	Lack of fit	R^2
Borosilicate glass	Contact angle	Actual equation $1.0/Y = 0.011374 - 1.22587E\text{-}003X_1 + 9.25626E\text{-}004X_1^2 - 1.24670E\text{-}004X_1^3$ Coded equation $1.0/y = 0.013 + 1.924E\text{-}003x_1 - 7.856E\text{-}004x_1^2 - 9.974E\text{-}004$	0.0006 (Significant)	0.0797 (Not significant)	0.8416
Stainless-steel	Contact angle	Actual equation $Y = 114.65007 - 15.60827X_1 - 3.42166X_2 + 1.52731X_1^2 + 0.13671X_2^2 + 1.06516X_1X_2 - 0.043267X_1X_2^2$ Coded equation $y = 79.82 + 0.22x_1 - 0.61x_2 + 6.11x_1^2 + 0.91x_2^2 - 0.38x_1x_2 - 11.44x_1x_2^2$	0.0004 (Significant)	0.1216 (Not significant)	0.9644

Table 4 describes the analysis of the coefficient for each model used to fit the contact angle data for the borosilicate glass and stainless-steel substrate. It was observed from **Table 4** that the PDMS concentration significantly affected the contact angle ($p < 0.05$)

 doi:10.20944/preprints202203.0307.v1

although the quadratic (x_{11}) and cubic (x_{111}) effects of the PDMS concentration were negative, which decreased the contact angle. In contrast, the quadratic effect of the PDMS concentration (x_{11}) for the stainless-steel substrate increased the contact angle but the interactive effect of both PDMS concentration and treatment time affected negatively the contact angle (x_{122}).

Table 4. Analysis of coefficients for the coded models used to fit the contact angle experimental data for the PDMS surface coating on borosilicate glass and stainless-steel substrates.

	Contact angle		
	Coefficient	**F**	**Prob < F**
BOROSILICATE GLASS			
Independent variables			
PDMS concentration, x_1	1.924E-003	18.10	0.0021
Treatment time, x_2	-	-	-
Interactions			
x_{11}	-7.856E-004	26.71	0.0006
x_{111}	-9.974E-004	12.16	0.0069
STAINLESS-STEEL			
Independent variables			
PDMS concentration, x_1	0.22	0.04	0.8467
Treatment time, x_2	-0.61	0.64	0.4548
Interactions			
x_{11}	6.11	55.04	0.0003
x_{12}	-0.38	0.12	0.7384
x_{22}	0.91	1.23	0.3094
x_{122}	-11.44	55.52	0.0003

Figure 3 shows the three-dimensional (3D) imaging of the response surface of the contact angle profiles for the borosilicate glass. Based on the cubic model with an inverse transformation, the contact angle of the borosilicate glass was only affected by the PDMS concentration without any interaction with the treatment time. The highest contact angle was recorded at low PDMS concentrations (1%, w/v) and decreased further with increasing PDMS concentration. The concentration of PDMS at 1% (w/v) was sufficient to increase the contact angle surface of the untreated borosilicate glass to become hydrophobic at 90–100° compared to initial contact angle before treatment, around 34°. Similar findings were previously reported (Ogihara *et al*., 2011) in which the increase in the silicon concentration through trimethyloxicilicate (TMSS) silicon showed no effect on the contact angle value of the copper substrate. While the surface remained hydrophilic without any TMSS, a small addition of TMSS caused the copper substrate to become superhydrophobic and increased the contact angle. On the other hand, the further addition of TMSS decreases the contact angle value (Ogihara *et al*., 2011). Likewise, Zhang *et al*. (2011) applied PDMS to treat the borosilicate crown optical glass surface to make it hydrophobic and increase the contact angle from 23.4° to 75.3°. Through a dehydration process, the PDMS removes the available hydroxyl groups and introduces hydrophobic methyl groups to the coating, thus, enhancing the hydrophobicity of the treated glass surface (Zhang *et al*., 2012).

Figure 4 shows the 3D plot of the response surface of the contact angle profiles for the stainless-steel substrate. The results showed that both the PDMS concentration and treatment time did not have a major impact on the surface of the substrate, as shown in **Table 4**. However, the interactive effect of these two factors, $x_1x_2^2$, was significant with negative coefficient values ($p < 0.05$). These findings revealed that the increase of PDMS concentration and the treatment time did not provide any significant improvement in the contact angle evaluation. In other words, the contact angle of the stainless-steel surface showed no substantial increase as the treatment time prolonged at low PDMS concentrations. In fact, the hydrophilicity of the stainless-steel surface was only maintained as the

 doi:10.20944/preprints202203.0307.v1

concentration of the PDMS increased at a short treatment time. Hence, the findings suggested that the stainless-steel surface's contact angle value would only increase at low PDMS concentration and shorter treatment time.

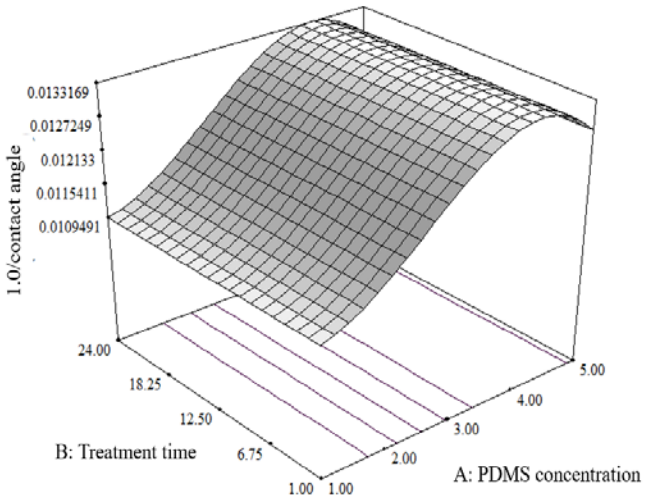

Figure 3. Response surface plot of PDMS concentration versus treatment time on the contact angle value of borosilicate glass.

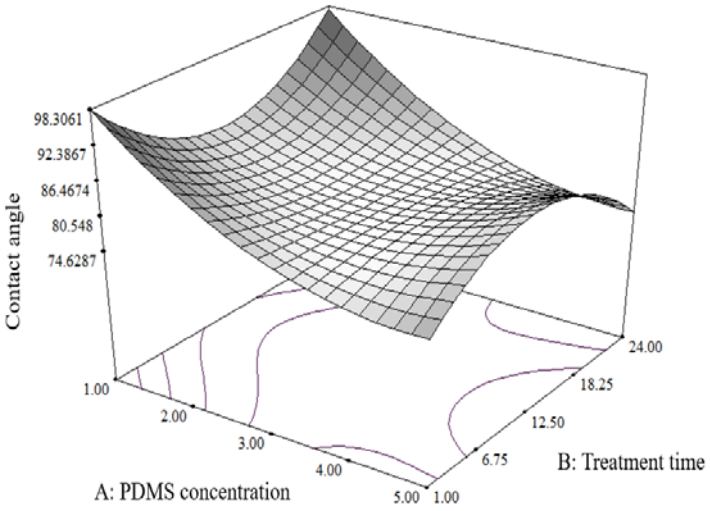

Figure 4. Response surface plot of PDMS concentration versus treatment time on the contact angle value of stainless-steel substrate.

Additionally, the treated stainless-steel surface had a lower degree of increment in contact angle compared to that of the borosilicate glass. Although the maximum contact angle of both substrates could reach nearly the same at 90–100°, the natural contact angle of the stainless-steel surface was higher (75.14°) compared to the borosilicate glass surface (32.51°). The characteristics of the stainless-steel hamper the ability of the PDMS solution to raise the contact angle of the stainless-steel surface (33% increase) to the same degree as the borosilicate glass surface (200% increase) from its normal contact angle. This was because the formation of the silanol group from the hydrolysis process in the PDMS solution formed an unstable condensation bond with the oxide group of iron or carbon. Moreover, the Si-O did not form stable bonds with alkaline metal oxides or carbonates (Arkles, 2014).

Preprints (www.preprints.org) | NOT PEER-REVIEWED | Posted: 23 March 2022 doi:10.20944/preprints202203.0307.v1

3.2. Determination of the Model Validity

The validity of the selected model was evaluated by repeating the tests to acquire the RMSD value, which represents the difference between the predicted and actual optimal points. The repetitive tests were carried out using the optimum parameter values according to the response surface analysis results. The calculated RMSD values using Equation 1 in **Table 5** obtained a small RMSD value (1.64) for the glass substrate and (3.37) for the stainless-steel substrate which validates the selected model.

Table 5. Comparison of the expected contact angle readings of the borosilicate glass and stainless-steel surfaces with actual contact angle measured in repeated trials with optimum parameters to determine model validity.

Substrate	Optimum PDMS concentration (%, v/v)	Optimum treatment time (hr)	Projected contact angle value (°)	Contact angle value from repeated experiment (°)			RMSD
				Replication 1	Replication 2	Replication 3	
Borosilicate glass	**1**	**4.92**	**90.91**	88.83	91.83	91.39	1.64
Stainless-steel	1	1	98.31	99.82	100.94	101.98	3.37

3.3. Surface Morphology of Borosilicate Glass and Stainless-steel Substrates

Figures 5(a) and **5(c)** depicts the surface structure variations of the borosilicate glass before being treated with the PDMS solution and **Figures 5(b)** and **5(d)** after being treated with the PDMS solution as observed under the FESEM at various magnification scales (1000X and 5000X from top to bottom). The observation in **Figure 5(b)** reveals that the chemical treatment with PDMS solution on the borosilicate glass caused a comprehensive morphological change of the substrate surface compared to its natural structure, as shown in **Figure 5(a)**.

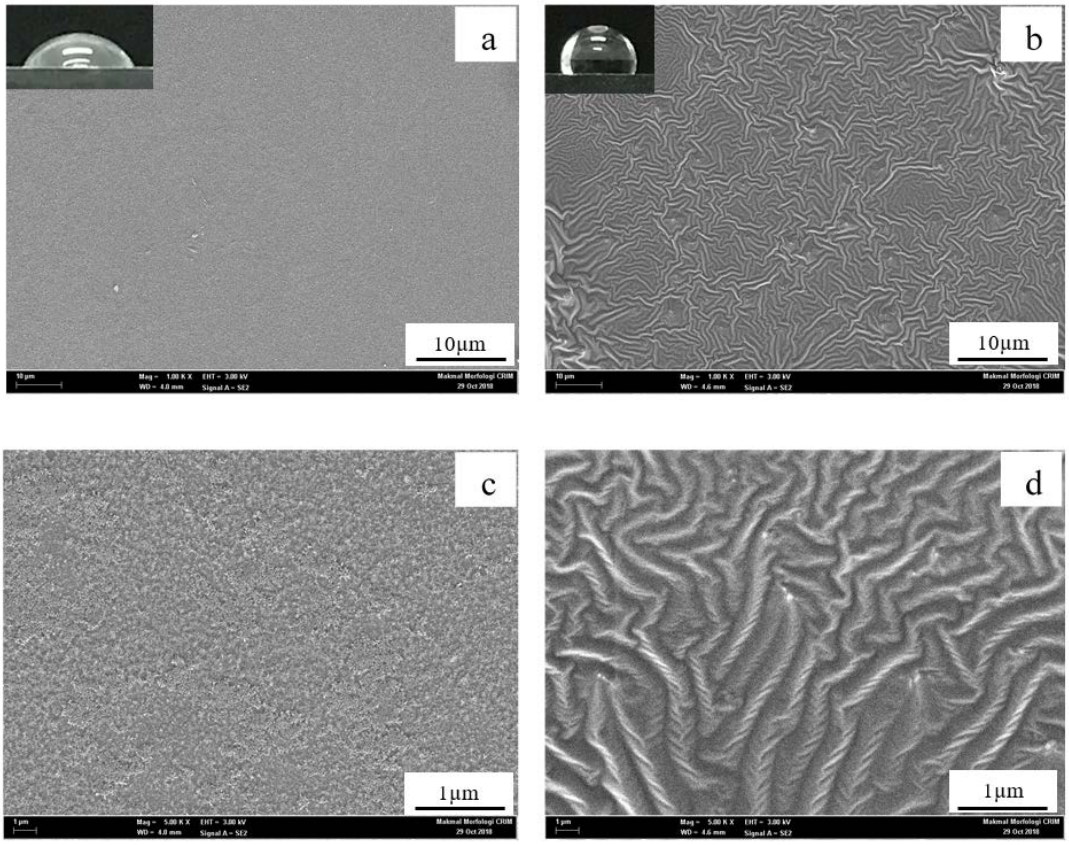

Figure 5. Surface morphology of borosilicate glass under (a) and (c) untreated conditions and (b) and (d) PDMS-treated conditions at different magnifications; (a) and (b) at 1000X magnification, (c) and (d) at 5000X magnification.

Preprints (www.preprints.org) | NOT PEER-REVIEWED | Posted: 23 March 2022 doi:10.20944/preprints202203.0307.v1

The surface of the borosilicate glass was hydrophilic since it was naturally rough with nanostructures. The hydrophilic property is contributed by the highly extensive contact between solids/liquids, which increases with the surface roughness of a material (Bodas & Khan-Malek, 2007). However, after the glass was treated with the PDMS solution, a layer of hydrophobic material from the PDMS solution covers the glass, which trapped more air on its surface and reduces the solids/liquid contact, resulting in a hydrophobic surface. The previous investigation also used SEM to study the structure of PDMS sheets treated with oxygen plasma and yielded a similar array of nanostructures (Bodas & Khan-Malek, 2007).

Aside from the roughness factor, any irregularities or the presence of holes on the surface should be considered when discussing the surface wetness qualities (Ashokkumar *et al*., 2012). **Figures 6(a)** and **6(c)** illustrate the FESEM images of untreated stainless-steel surfaces at 1000X and 5000X magnification, while **Figures 6(b)** and **6(d)** show the FESEM imaging of treated stainless-steel surfaces with PDMS solutions. **Figure 6(a)** depicts the surface of natural stainless-steel before treatment, with no PDMS solution applied. The surface morphology of borosilicate glass treated with PDMS solution was distinguished by the presence of many grooves and curves, which demonstrated significant surface morphology differences compared to the relatively flattened surface of the untreated borosilicate glass. Previous SEM examination of zinc-coated steel surface with functional silicon revealed the presence of holes that were etched on the sample surface, allowing the microstructure to trap huge amounts of air and making the surface superhydrophobic (Brassard *et al*., 2015).

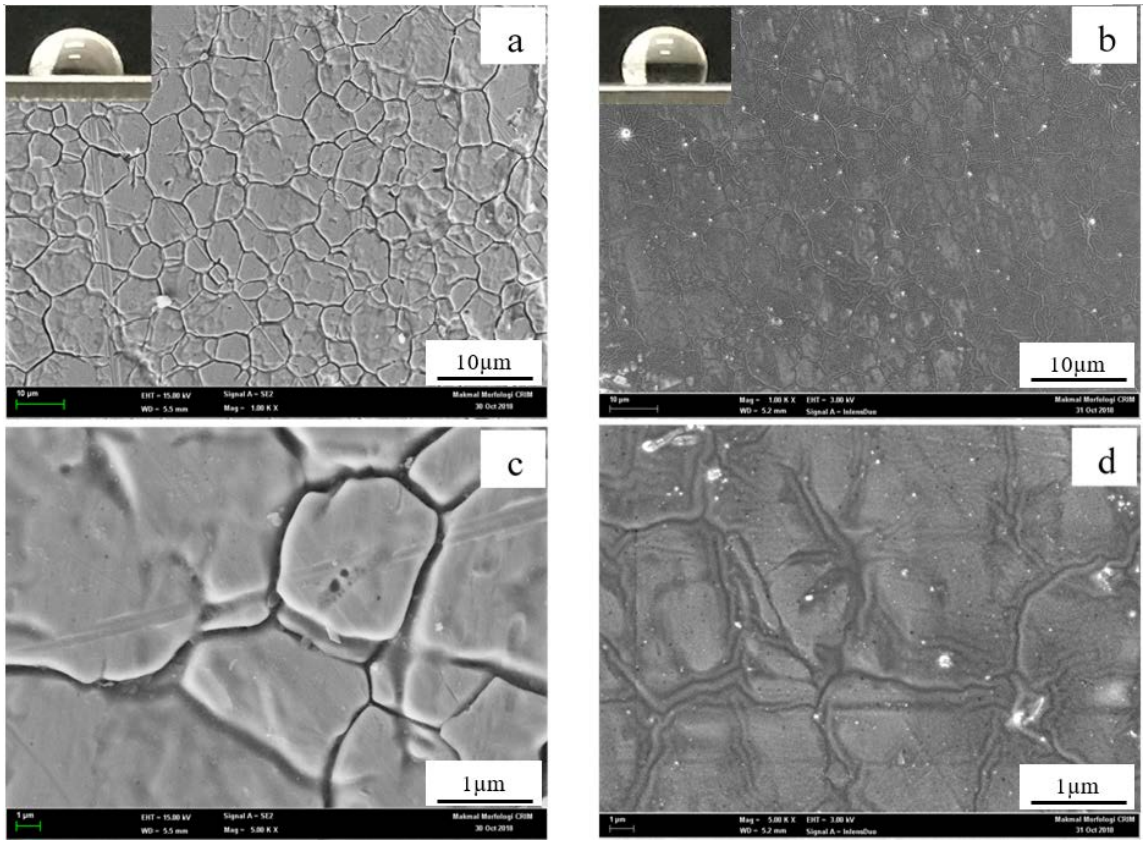

Figure 6. Surface morphology of stainless-steel substrates under (a) and (c) untreated conditions and (b) and (d) PDMS-treated conditions at different magnifications; (a) and (b) at 1000X magnification, (c) and (d) at 5000X magnification.

Furthermore, the addition of a thin layer of diluted PDMS solution increased the contact angle value of the stainless-steel surface from 75.14° to 104°. The hydrophobic

 doi:10.20944/preprints202203.0307.v1

characteristics of the treated surface were based on the Cassie-Baxter model, which states that the low wettability is due to the formation of the rough nano-sized arrangement covered by a hydrophobic substance with air trapped in its topography (Cassie & Baxter, 1944).

3.4. Determination of Functional Groups on the Surface of Borosilicate Glass and Stainless-steel Substrates

The FTIR spectra were examined in the region of 4000–650 cm^{-1} to analyse the changes in the chemical structure of the substrate surface. The FTIR spectra of untreated borosilicate glass in **Figure 7** revealed individual peaks at 767 cm^{-1} and 918 cm^{-1} that corresponds to Si-O-Si and Si-O- groups, respectively (Abenojar *et al*., 2013). The absence of a peak at 1259 cm^{-1} demonstrated that PDMS was not present on the surface of untreated borosilicate glass (Yu, 2014). On the contrary, the obtained spectra on the surface of borosilicate glass treated with PDMS indicated the presence of additional peaks, notably Si-O-Si (1008 cm^{-1}), Si-CH_3 (1259 cm^{-1}), and CH_2 and CH_3 (2854 cm^{-1}, 2927 cm^{-1}, and 2962 cm^{-1}) (Ting *et al*., 2014).

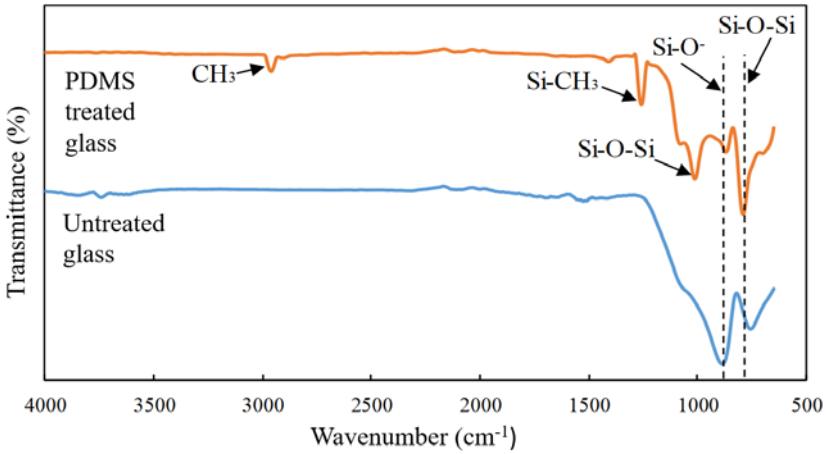

Figure 7. FTIR spectra of untreated and PDMS-treated borosilicate glass surfaces.

The considerable drop in the Si-O- concentration peak as well as the increase in Si-O-Si concentration across the surface spectrum of treated borosilicate glass could be attributed to the changes in the functional group of borosilicate glass surfaces from Si-O- bonds to Si-O bonds -Si (Abenojar *et al*., 2013). The hydrophobic radicals that caused the surface of the glass substrate to change properties comprising Si-CH_3, CH_2, and CH_3 were formed as the result of the breakdown of the PDMS solution. Consequently, these radicals react with the borosilicate glass to form a hydrophobic coating (Fang *et al*., 2004).

The prominent peaks at 1006 cm^{-1} were attributed to the Si-O-Si bonds as a result of the stretching motion of the Si-O-Si bridge. Due to the action of silanol, the peaks were subsequently split into two bands at 1043 cm^{-1} and 1006 cm^{-1}, as obtained in the previous work (Mahadik *et al*., 2010). These two distinct peaks are frequently identified in oligomers, polymers, and PDMS networks (Guermeur *et al*., 1999). The presence of this peak supports the formation of the Si-O-Si network produced through the addition of the PDMS solution. Based on the FTIR data, it was deduced that the Si-O-Si networks were developed on the surface of PDMS-treated borosilicate glass, which contributes to the hydrophobic characteristics of the borosilicate glass surface.

As shown in **Figure 8**, the FTIR-ATR evaluation of PDMS-treated stainless-steel surfaces revealed the spinal structure of the -Si $(CH_3)_2$-O- network, which was indicated in the PDMS spectrum by a band that is typical of PDMS. According to the findings, certain differences in peak heights were visible before and after the PDMS treatment. Several weak peaks were identified at 871 cm^{-1} and 791 cm^{-1} on the PDMS-treated stainless-steel

Preprints (www.preprints.org) | NOT PEER-REVIEWED | Posted: 23 March 2022 doi:10.20944/preprints202203.0307.v1

surface, which were caused by the Si-C vibration and CH_3 motion of the $SiCH_3$ group, respectively (Yousefi *et al*., 2017). Similarly, the Si-O-Si band was represented by the peaks at 1095 cm^{-1} and 1017 cm^{-1}. Meanwhile, asymmetrical C-H bending was responsible for the new peak at 1245 cm^{-1}, while the apex of the methyl group's stretching motion was linked with a faint band at 2985 cm^{-1}. Following that, a strip at the peak of 3480 cm^{-1} was produced by a hydroxyl group that was not available on the untreated stainless-steel surface (Su *et al*., 2017). All peaks at 791, 1017, 1095, 1245, and 2968 cm^{-1} demonstrated the significant presence of PDMS groups on the surface of the treated substrate (Yousefi *et al*., 2017).

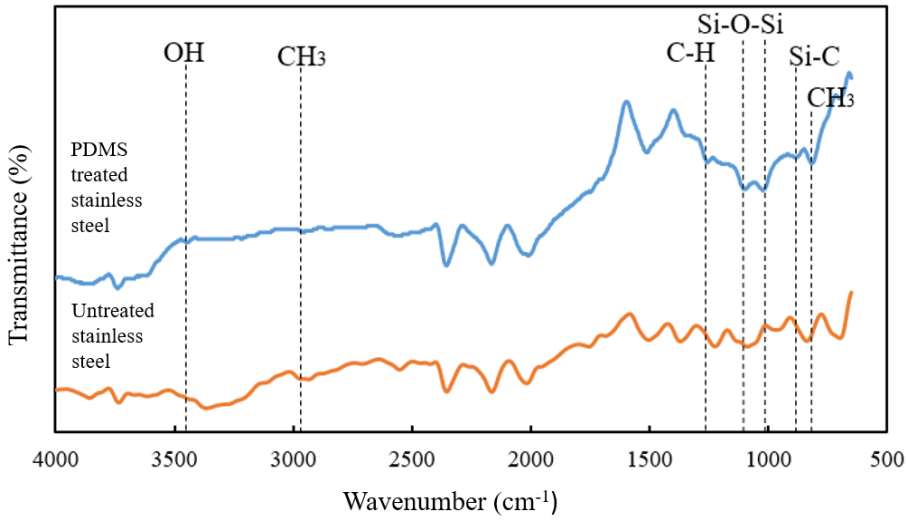

Figure 8. FTIR spectra of untreated and PDMS-treated stainless-steel surfaces.

4. Conclusion

This study demonstrated the successful use of PDMS solution to form a hydrophobic surface on borosilicate glass and stainless-steel substrates. The applied surface treatment increased the contact angle between the two surfaces, therefore, altering their nature to become more hydrophobic. Based on the RSM analysis, the PDMS concentration had a greater effect compared to the treatment period on the contact angle of the borosilicate glass, while both parameters had a negative interaction effect on the stainless-steel substrate. At low PDMS concentrations, both substrates exhibited excellent hydrophobic characteristics, which achieved the highest contact angle increment ranging from 90–100°. In comparison, the PDMS solution was more effective on the borosilicate glass than on the stainless-steel surface, as indicated by the percentage increase of the contact angle measurement. The FESEM micrograph in this study also revealed the presence of nanostructures that traps the air between the hydrophobic layers, hence, boosting the water repellent capacity. Furthermore, the FTIR examination showed the development of new peaks on the substrate surface, notably Si-O-Si, $Si-CH_3$, CH_2, and CH_3, indicating the presence of interaction between the PDMS solution and the substrate surface. Overall, the study presented a simple and economical approach with no specialised equipment or harsh processing conditions for an appropriate surface treatment via spray dryer application to alleviate the product adhesion issues as the transition from hydrophilic to hydrophobic surface qualities was effectively accomplished.

Acknowledgements

We are grateful to Universiti Kebangsaan Malaysia (UKM) for the financial support (GUP-2018-057; GUP-2018-080), the Ministry of Higher Education of Malaysia (FRGS/1/2020/WAB04/UKM/02/4), and the Department of Food Sciences, Faculty of

Science and Technology, UKM for allowing this study to be carried out at their Food Pilot Plant.

Data Availability Statement

No data were used elsewhere to support this study and it was entirely a new set of data.

References

Abenojar, J., Martínez, M. a., Encinas, N. & Velasco, F. 2013. Modification of glass surfaces adhesion properties by atmospheric pressure plasma torch. *International Journal of Adhesion and Adhesives* 44: 1–8.

Arkles, B. 2014. Silane Coupling Agents: Connecting Across Boundaries. Morrisville, PA: Gelest, Inc.

Arkles, B. 2015. Hydrophobicity, Hydrophilicity and Silane Surface Modification. Morrisville, PA: Gelest, Inc. DOI:10.1017/CBO9781107415324.004

Ashokkumar, S., Adler-Nissen, J. & Moller, P. 2012. Factors affecting the wettability of different surface materials with vegetable oil at high temperatures and its relation to cleanability. *Applied Surface Science* 263: 86–94.

Bhandari, B. & Howes, T. 2005. Relating the Stickiness Property of Foods Undergoing Drying and Dried Products to their Surface Energetics. *Drying Technology* 23(4): 781–797.

Bodas, D. & Khan-Malek, C. 2007. Hydrophilization and hydrophobic recovery of PDMS by oxygen plasma and chemical treatment-an SEM investigation. *Sensors and Actuators, B: Chemical* 123(1): 368–373.

Brassard, J. D., Sarkar, D. K., Perron, J., Audibert-Hayet, A. & Melot, D. 2015. Nano-micro structured superhydrophobic zinc coating on steel for prevention of corrosion and ice adhesion. *Journal of Colloid and Interface Science* 447: 240–247.

Cassie, A. B. D. & Baxter, S. 1944. Wettability of porous surfaces. *Transactions of the Faraday Society* 40: 546–551.

El Dessouky, W. I., Abbas, R., Sadik, W. A., El Demerdash, A. G. M. & Hefnawy, A. 2017. Improved adhesion of superhydrophobic layer on metal surfaces via one step spraying method. *Arabian Journal of Chemistry* 10(3): 368–377.

Fang, Z., Qiu, Y. & Kuffel, E. 2004. Formation of hydrophobic coating on glass surface using atmospheric pressure non-thermal plasma in ambient air. *Journal of Physics D: Applied Physics* 37(16): 2261.

Fang, Z. & Bhandari, B. 2012. Comparing the efficiency of protein and maltodextrin on spray drying of bayberry juice. *Food Research International* 48(2): 478–483.

Guermeur, C., Lambard, J., Gerard, J.-F. & Sanchez, C. 1999. Hybrid polydimethylsiloxane-zirconium oxo nanocomposites. Part 1 Characterization of the matrix and the siloxane-zirconium oxo interface. *Journal of Materials Chemistry* 9(3): 769–778.

Huang, K. & Goddard, J. M. 2015. Influence of fluid milk product composition on fouling and cleaning of Ni-PTFE modified stainless steel heat exchanger surfaces. *Journal of Food Engineering* 158: 22–29.

Katsoulis, D. E., Schmidt, R. G. & Zank, G. A. 2017. Siloxanes and silicones. in Lee (ed.). Advances in Silicone Technologies 2000–15, p. 301–322. Midland US: Academic Press.

Mahadik, S. A., Kavale, M. S., Mukherjee, S. K. & Rao, A. V. 2010. Transparent superhydrophobic silica coatings on glass by sol-gel method. *Applied Surface Science* 257(2): 333–339.

Ogihara, H., Katayama, T. & Saji, T. 2011. One-step electrophoretic deposition for the preparation of superhydrophobic silica particle/trimethylsiloxysilicate composite coatings. *Journal of Colloid and Interface Science* 362(2): 560–566.

Piñeiro, G., Perelman, S., Guerschman, J. P. & Paruelo, J. M. 2008. How to evaluate models: Observed vs. predicted or predicted vs. observed? *Ecological Modelling* 216(3): 316–322.

Sari, A. M. 2006. The effect of teflon liquid sprayed silicate glass coating on improving its hydrophobicity. *Prosiding Simposium Nasional Polimer*, p .98–104. *Simposium Nasional Polimer*. DOI: ISSN 1410-8720

Schuck, P., Méjean, S., Dolivet, A. & Jeantet, R. 2005. Thermohygrometric sensor: A tool for optimizing the spray drying process. *Innovative Food Science & Emerging Technologies* 6(1): 45–50.

 doi:10.20944/preprints202203.0307.v1

Su, X., Li, H., Lai, X., Zhang, L., Liang, T., Feng, Y. & Zeng, X. 2017. Polydimethylsiloxane-based surfaces on steel substrate: Fabrication, reversibly extreme wettability and oil–water separation. *ACS Applied Materials & Interfaces* 9(3): 3131–3141.

Ting, J. A. S., Rosario, L. M. D., Lee, H. V., Ramos, H. J. & Tumlos, R. B. 2014. Hydrophobic coating on glass surfaces via application of silicone oil and activated using a microwave atmospheric plasma jet. *Surface and Coatings Technology* 259: 7–11.

Wang, S., Li, Y., Fei, X., Sun, M., Zhang, C., Li, Y. & Yang, Q. 2011. Preparation of a durable superhydrophobic membrane by electrospinning poly(vinylidene fluoride) (PVDF) mixed with epoxy – siloxane modified SiO_2 nanoparticles : A possible route to superhydrophobic surfaces with low water sliding angle and high water contact angle. *Journal of Colloid and Interface Science* 359(2): 380–388.

Wang, F., Wang, X., Xie, A., Shen, Y., Duan, W., Zhang, Y. & Li, J. 2012. A simple method for preparation of transparent hydrophobic silica-based coatings on different substrates. *Applied Physics A: Materials Science and Processing* 106(1): 229–235.

Woo, M. W., Daud, W. R. W., Tasirin, S. M. & Talib, M. Z. M. 2009. Controlling food powder deposition in spray dryers : Wall surface energy manipulation as an alternative. *Journal of Food Engineering* 94(2): 192–198.

Yousefi, M., Zerafat, M., Shokri Doodeji, M. & Sabbaghi, S. 2017. Investigation of dip-coating parameters effect on the performance of alumina-polydimethylsiloxane nanofiltration membranes for desalination. *Journal Water Environment Nanotechnology* 2(4): 235–242.

Yu, L. 2014. The adhesion of poly(dimethyl siloxane) to silica substrates. McMaster University.

Yu, M., Liu, F. & Du, F. 2016. Synthesis and properties of a green and self-cleaning hard protective coating. *Progress in Organic Coatings* 94: 34–40.

Zhang, Y., Zhang, X., Ye, H., Xiao, B., Yan, L. & Jiang, B. 2012. A simple route to prepare crack-free thick antireflective silica coatings with improved antireflective stability. *Materials Letters* 69: 86–88.